Article

A Unifying Synthesis Approach to the C18#, C19#, and C20#Diterpenoid Alkaloids

Kevin G. M. Kou, Svitlana Kulyk, Christopher J Marth, Jack C. Lee, Nicolle A Doering, Beryl X. Li, Gary M. Gallego, Terry P Lebold, and Richmond Sarpong

Just Accepted

A Unifying Synthesis Approach to the C$_{18}$–, C$_{19}$–, and C$_{20}$–Diterpenoid Alkaloids

Kevin G. M. Kou, Svitlana Kulyk,[†] Christopher J. Marth,[‡] Jack C. Lee,[§] Nicolle A. Doering, Beryl X. Li, Gary M. Gallego,[¶] Terry P. Lebold[‖] and Richmond Sarpong*

Department of Chemistry, University of California, Berkeley, California 94720, United States

ABSTRACT: The secondary metabolites that comprise the diterpenoid alkaloids are categorized into C$_{18}$-, C$_{19}$-, and C$_{20}$-families depending on the number of contiguous carbon atoms that constitute their central framework. Herein, we detail our efforts to prepare these molecules by chemical synthesis, including a photochemical approach, and ultimately a bioinspired strategy that has resulted in the development of a unifying synthesis of one C$_{18}$ (weisaconitine D), one C$_{19}$ (liljestrandinine), and three C$_{20}$ (cochlearenine, paniculamine, and N-ethyl-1α-hydroxy-17-veratroyldictyzine) natural products from a common intermediate.

INTRODUCTION

The diterpenoid alkaloids are complex, bridged, polycyclic natural products that possess analgesic, anti-inflammatory, anti-arrhythmic, and other pharmacological activities.[1–3] The *Aconitum*, *Consolidum*, and *Delphinium* plants from which these pseudoalkaloids are isolated have long been used in traditional medicine for the treatment of pain and cardiovascular diseases. In fact, Guan-fu base A (**5**, Figure 1) is in phase IV clinical trials as an anti-arrhythmic agent in China,[4] while the hydrobromide salt of lappaconitine (**1**) is approved and marketed in both China and Russia as a pain and arrhythmia treatment.[5] Perhaps most intriguing is the ability of some diterpenoid alkaloids to modulate Na$^+$ and/or K$^+$ ion channels.[6] For example, aconitine (**3**) is a highly toxic Na$^+$ channel activator with an estimated lethal dose of 1–2 mg in humans.[7] However, structurally related lappaconitine (**1**) is a Na$^+$ channel blocker that has therapeutic value.[6] The potential for these molecules to act as subtype-selective ion channel modulators has significant implications for treating channelopathies without significant undesirable side effect profiles.[8,9] While over 1200 members make up this class of secondary metabolites, few have been studied for their function due to inadequate accessibility. Developing synthesis strategies that allow access to a variety of these natural products and related unnatural analogs would facilitate structure-activity-relationship studies and provide myriad opportunities for clinical applications.

Attracted by the challenges associated with the architectural complexity, and the opportunities to learn about the biological function of these natural products, we embarked on a total synthesis campaign targeting members of the C$_{18}$-, C$_{19}$-, and C$_{20}$-diterpenoid alkaloids[5,10,11] with varying substitution and oxygenation patterns decorating their framework. These efforts have led to the first syntheses of

weisaconitine D (C$_{18}$, **2**), liljestrandinine (C$_{19}$, **4**), cochlearenine (C$_{20}$, **6**), N-ethyl-1α-hydroxy-17-veratroyldictyzine (C$_{20}$, **7**), and paniculamine (C$_{20}$, **8**).[12,13]
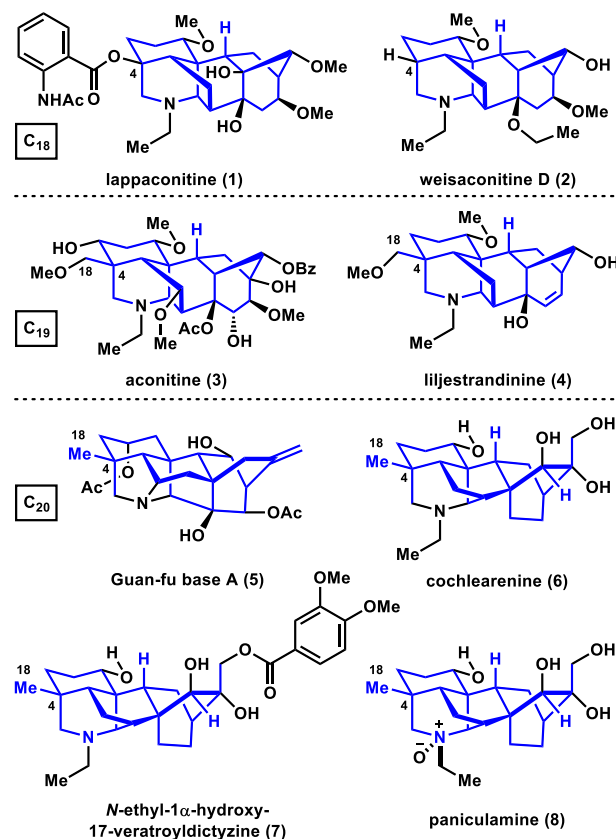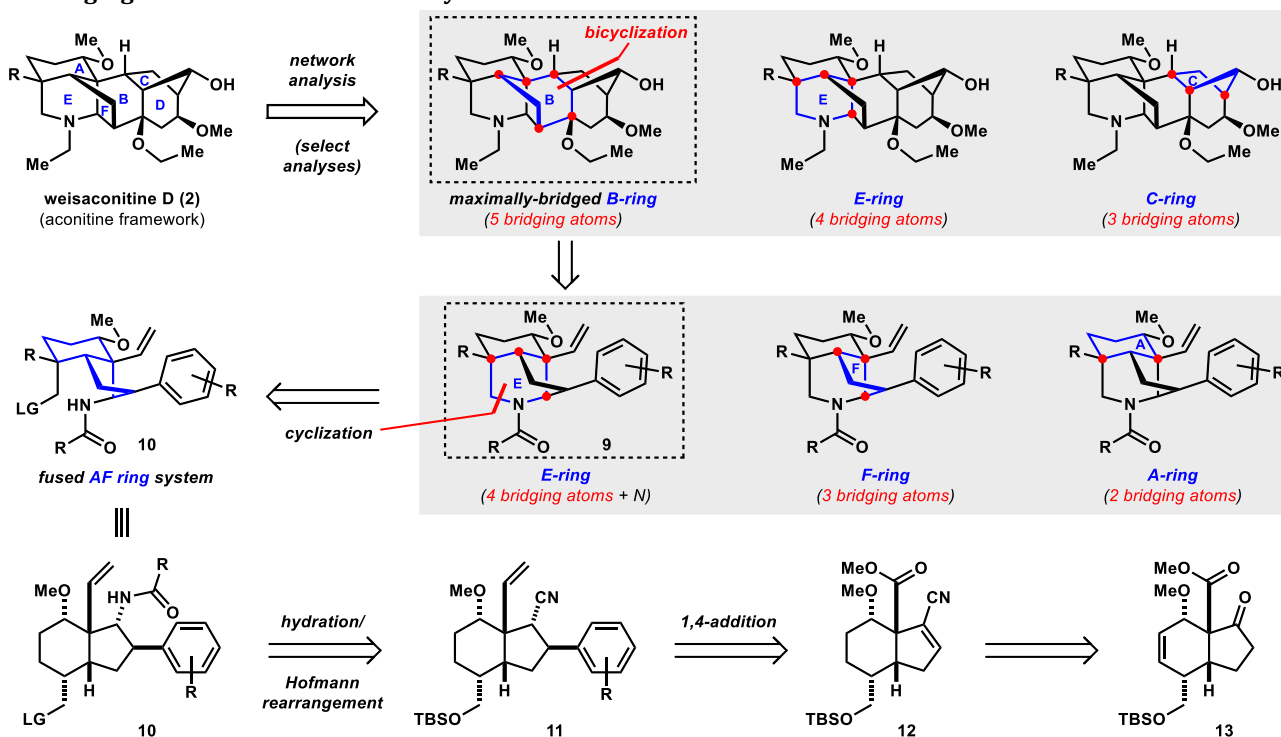

Figure 1. Examples of diterpenoid alkaloids.

Scheme 1. Network-analysis-guided retrosynthetic analysis of aconitine-type natural products. The red dots indicate bridging atoms in the network analyses

network analysis

(select analyses)

weisaconitine D (2)
(aconitine framework)

bicyclization

maximally-bridged B-ring
(5 bridging atoms)

E-ring
(4 bridging atoms)

C-ring
(3 bridging atoms)

cyclization

10

fused AF ring system

E-ring
(4 bridging atoms + N) **9**

F-ring
(3 bridging atoms)

A-ring
(2 bridging atoms)

hydration/

Hofmann rearrangement

10

11

1,4-addition

12

13

RESULTS AND DISCUSSION

The assembly of these structurally complex molecules has challenged synthetic chemists since the 1960's, beginning with Nagata, Masamune, and Wiesner's formal syntheses[14] of C_{20}-members atisine,[15] garryine,[16,17] and viatchine.[17,18] While lengthy, these contributions set the stage for the field and provided inspiration even to modern synthetic approaches, including our own (see Scheme 7).[19,20] Recently, the Baran and Xu groups have devised unified strategies toward various diterpenoid alkaloids but particularly natural products within the C_{20} family.[21,22] Our group demonstrated conversion of the C_{20} hetidine core to the atisine framework,[23,24] and the Fukuyama group subsequently showed that an advanced intermediate used enroute to the C_{20} natural product (−)-lepenine[25] can also be used to synthesize the C_{19} alkaloid (−)-cardiopetaline.[26] Here we describe our studies on an approach that unifies the syntheses of secondary metabolites belonging to each of the C_{18}, C_{19}, and C_{20} families.

Retrosynthesis. For bridged, polycyclic molecules with complexity as daunting as that of the diterpenoid alkaloids, network analysis, an approach formalized by Corey,[27] provides an objective starting point and guide for retrosynthetic analyses. In a complex molecular setting containing a network of fused and bridged-ring systems, the latter are generally perceived to be more challenging to assemble. However, significant simplification to the network can be achieved by iteratively cleaving bonds associated with the maximally bridged ring(s), which is a key element of network analysis.

In applying network analysis to the hexacyclic aconitine framework, as exemplified by weisaconitine D (Scheme 1), each of the individual rings can be analyzed for the number of bridging atoms (or bridgehead sites) that they contain.
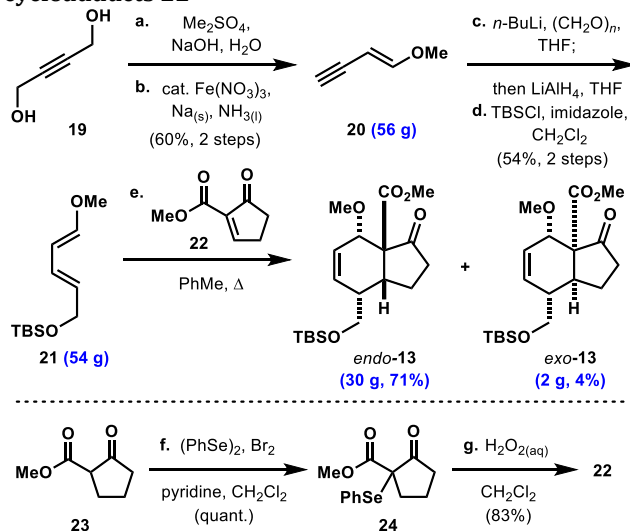
In this case, the B-ring contains five bridging atoms, the E- and F-rings four bridging atoms (F-ring not shown, see SI), the C-ring contains three bridging atoms, the D-ring three bridging atoms (not shown), and the A-ring two bridging atoms (not shown). Having identified the B-ring as the maximally-bridged ring, we envisioned a bicyclization transform that effectively simplifies the target to tricyclic vinyl arene **9**. In the forward sense, this operation forges two bonds and three new rings in a single step.[28] Similarly, applying network analysis to intermediate **9** yields the piperidine E-ring as the maximally-bridged system with four bridging atoms. Since the piperidine ring also contains a nitrogen atom (a functional group), we reasoned that its disconnection would provide the greatest simplification, thus leading back to fused AF ring system **10** that contains no bridging elements. The protected amine functionality of **10** can arise from a hydration and Hofmann rearrangement sequence on nitrile **11**, which in turn can be prepared from vinyl nitrile **12** through a conjugate arylation reaction and transformation of the methyl ester. This intermediate can be further simplified to hydrindenone **13**, which can be accessed in >20 g quantities using a Diels–Alder reaction.[13]

Correctly identifying the maximally-bridged ring systems in complex polycycles manually is inherently time-consuming.[29,30] Therefore, to facilitate the use of network analysis in retrosynthetic planning,[31] we developed a computer algorithm that correctly identifies the maximally-bridged ring(s) for any molecule using the Chemistry Development Kit software library.[12,32–34] We envision this web-based deterministic program to be a useful tool in both the research laboratory and classroom for retrosynthesis and chemical education.

Scheme 2. Proposed meta-π-arene photocycloaddition approach to the BCD ring system

14   *exciplex*

15   **16**   [O]

17   **18**
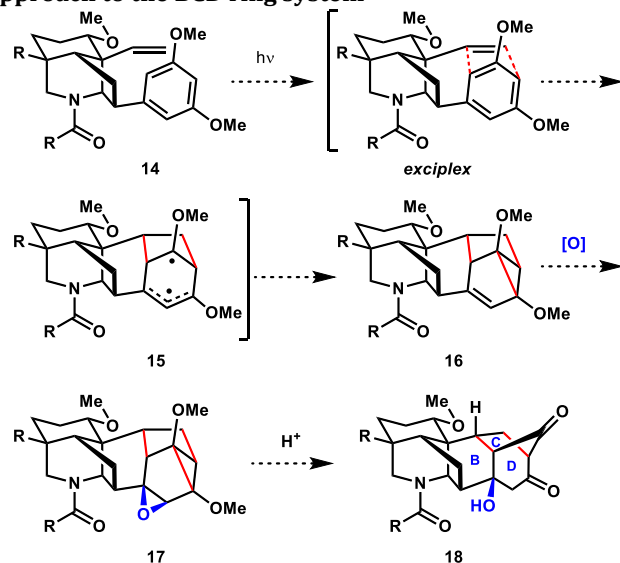
Scheme 3. Decagram-scale synthesis of diene 20 and cycloadducts 22

19

a. Me$_2$SO$_4$, NaOH, H$_2$O

b. cat. Fe(NO$_3$)$_3$, Na$_{(s)}$, NH$_{3(l)}$ (60%, 2 steps)

20 (56 g)

c. *n*-BuLi, (CH$_2$O)$_n$, THF; then LiAlH$_4$, THF

d. TBSCl, imidazole, CH$_2$Cl$_2$ (54%, 2 steps)

21 (54 g)

e. **22** MeO PhMe, Δ

endo-13 (30 g, 71%)   +   **exo-13 (2 g, 4%)**

23

f. (PhSe)$_2$, Br$_2$ pyridine, CH$_2$Cl$_2$ (quant.)

24

g. H$_2$O$_{2(aq)}$ CH$_2$Cl$_2$ (83%)

22

a Reaction conditions: (a) Me$_2$SO$_4$, NaOH, H$_2$O, 90–100 °C; (b) NH$_{3(l)}$, Fe(NO$_3$)$_3$·9H$_2$O (cat.), Na$_{(s)}$, 60% over two steps; (c) *n*-BuLi, THF, −78 to 23 °C, then (CH$_2$O)$_n$, 0–23 °C, then LiAlH$_4$, 0–23 °C; (d) TBSCl, imidazole, CH$_2$Cl$_2$, 23 °C, 54% over two steps; (e) diene **21**, dienophile **22**, PhMe, 100 °C, 71% *endo*-**13** + 4% *exo*-**13**, (f) (PhSe)$_2$, Br$_2$, pyridine, CH$_2$Cl$_2$, quant; (g) H$_2$O$_{2(aq)}$, CH$_2$Cl$_2$, 0–23 °C, 83%.
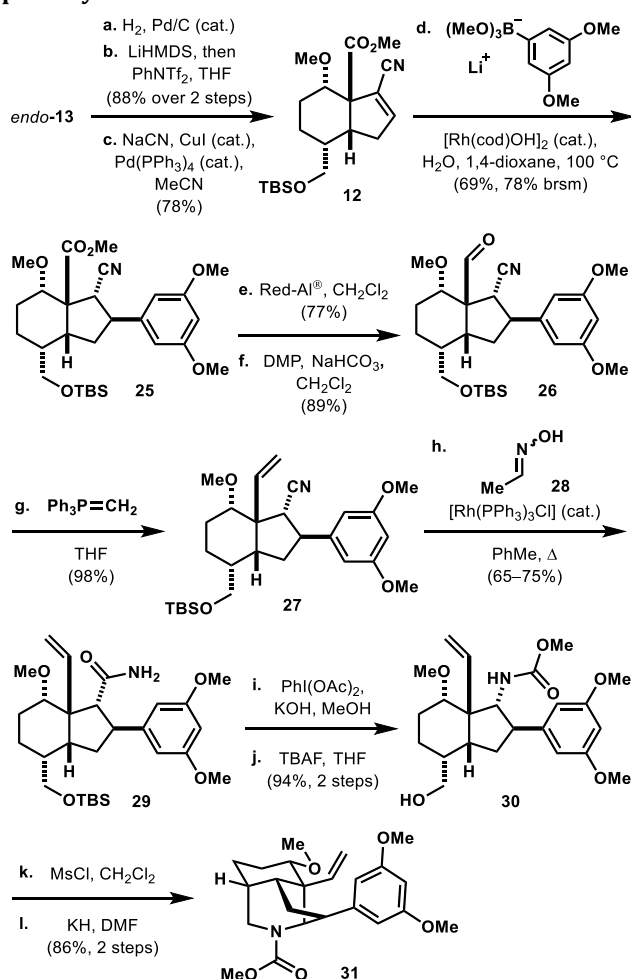
A photochemical approach to the CD [3.2.1] bicyclic ring system. Using network analysis, we determined that a bicyclization reaction to form the BCD ring systems would be most effective in directly assembling the target hexacyclic structure. To achieve this, we imagined a late-stage meta-π-arene photocycloaddition between the alkene and arene groups of vinyl arene **14** (Scheme 2). Photoexcitation of the arene component with UV irradiation was expected to lead to formation of an exciplex where concerted σ-bond formations would occur to generate diradical **15**. Spontaneous collapse of the diradical intermediate would form vinyl cyclopropane **16**.[35] Subsequent oxidation of the alkene to epoxide **17** could be followed by an acid-mediated cyclopropane fragmentation and epoxide

ring-opening to furnish diketone **18**.[36,37] This approach would be unlike the proposed biosynthesis of the lappaconitine and aconitine-type diterpenoid alkaloids that contain the [3.2.1]-CD bicyclic structure, and would provide a more direct route to the desired carbon framework.

We chose to introduce a methoxy-substituted aromatic ring (see **14**) because the arene oxygens would be native to many of our target natural products. In addition, electron-rich methoxy groups direct meta-π-functionalization to sites ortho to them, which would permit us to take maximum advantage of the substituents inherent to the target structures, thereby streamlining synthesis.

The synthesis begins with dimethylation of 1,4-butynediol (**19**, Scheme 3) followed by NaNH$_2$-promoted elimination/isomerization to generate enyne **20** in 60% yield.[38] A two-step sequence involving alkylation of the terminal alkyne with paraformaldehyde and subsequent

Scheme 4. Synthesis of vinyl arene intermediate 31 for photocycloaddition

endo-**13**

a. H$_2$, Pd/C (cat.)
b. LiHMDS, then PhNTf$_2$, THF (88% over 2 steps)
c. NaCN, CuI (cat.), Pd(PPh$_3$)$_4$ (cat.), MeCN (78%)

12

d. (MeO)$_3$B⁻ Li⁺
[Rh(cod)OH]$_2$ (cat.), H$_2$O, 1,4-dioxane, 100 °C (69%, 78% brsm)

25

e. Red-Al®, CH$_2$Cl$_2$ (77%)
f. DMP, NaHCO$_3$, CH$_2$Cl$_2$ (89%)

26

g. Ph$_3$P=CH$_2$ THF (98%)

27

h. [Rh(PPh$_3$)$_3$Cl] (cat.) PhMe, Δ (65–75%)

28

29

i. PhI(OAc)$_2$, KOH, MeOH
j. TBAF, THF (94%, 2 steps)

30

k. MsCl, CH$_2$Cl$_2$
l. KH, DMF (86%, 2 steps)

31

a Reaction conditions: (a) H$_2$, Pd/C (cat.), EtOAc, 23 °C; (b) LiHMDS, then PhNTf$_2$, THF, −78 to 23 °C, 88% over two steps; (c) NaCN, CuI (cat.), Pd(PPh$_3$)$_4$ (cat.), MeCN, 78%; (d) aryl boronic ester (prepared from the corresponding ArBr, *n*-BuLi, Et$_2$O, −78 to 23 °C; then B(OMe)$_3$, −40 °C); then **12**, [Rh(cod)OH]$_2$ (cat.), H$_2$O, 1,4-dioxane, 100 °C, 69%; (e) Red-Al®, CH$_2$Cl$_2$, 0–23 °C, 77%, (f) DMP, NaHCO$_3$, CH$_2$Cl$_2$, 89%; (g) PPh$_3$MeBr, LiHMDS, THF, 70 °C; then **26**, 0–23 °C, 98%; (h) **28**, [Rh(PPh$_3$)$_3$Cl] (cat.), PhMe, 130 °C, 65–75%; (i) PhI(OAc)$_2$, KOH, MeOH, 94%; (j) TBAF, THF, 23 °C, 94% over two steps; (k) MsCl, CH$_2$Cl$_2$; (l) KH, DMF, 60 °C, 86% over two steps. TBAF = tetrabutylammonium fluoride.

Scheme 5. Exploring alkene-arene photocycloadditions
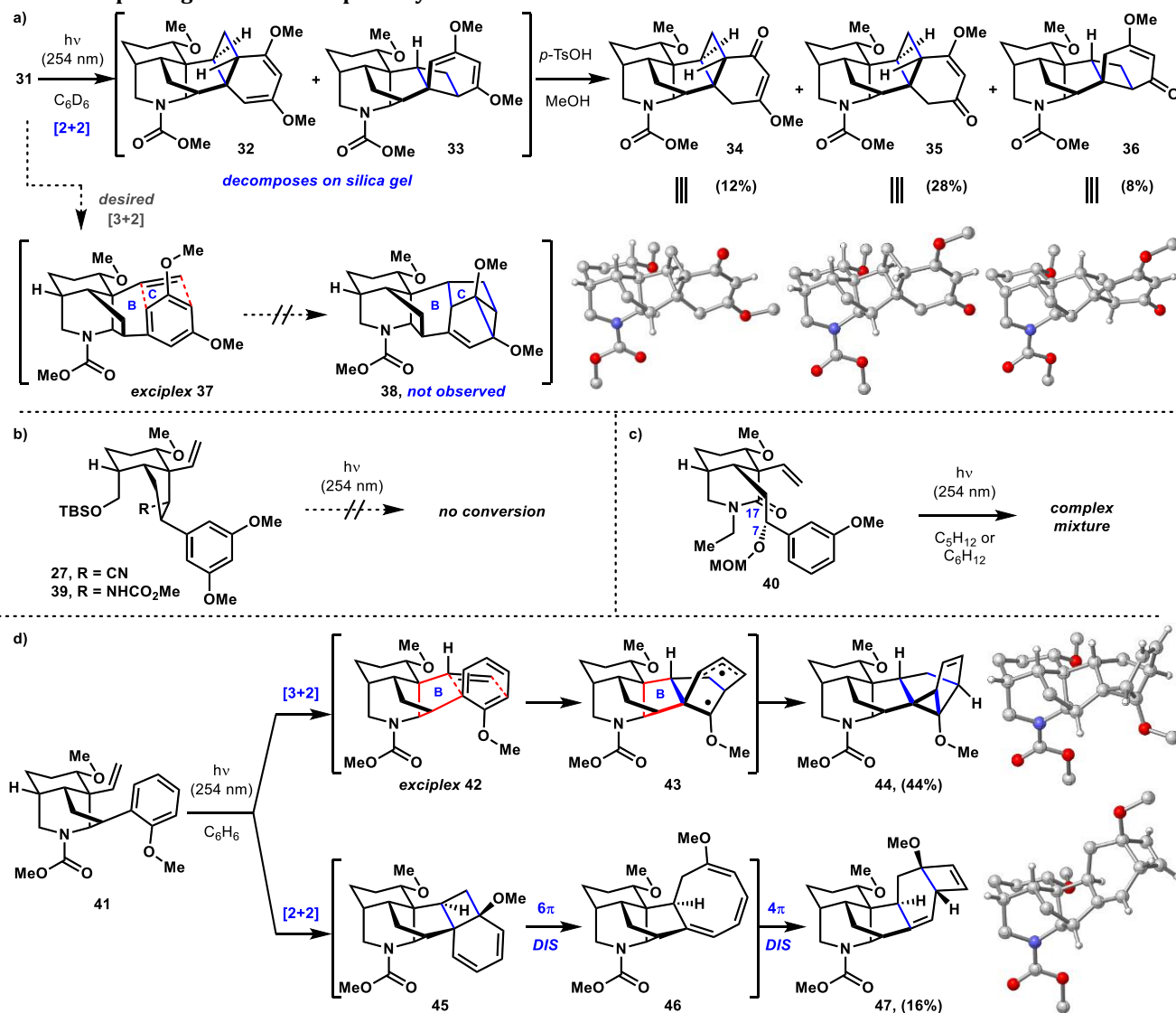
reduction of the propargyl alkyne with LiAlH$_4$, followed by TBS-protection of the primary alcohol yields diene **21**,[39] which can be prepared on 54 g scale in a single pass. Heating a two-equivalent excess of diene **21** with dienophile **22** (prepared from α-selenation of β-ketoester **23**, followed by selenoxide elimination from **24**)[40] results in formation of the desired *endo*-cycloadduct (**13**) as the major product in 71% yield, along with the *exo*-diastereomer in 4% yield.

The alkene group in hydrindenone *endo*-**13** is hydrogenated with Pd/C as the catalyst, and the ketone group converted to the vinyl triflate by treatment with LiHMDS and PhNTf$_2$ in 88% yield over the two steps (Scheme 4). The resulting vinyl triflate is then converted to vinyl nitrile **12** in 78% yield by a Pd- and Cu-catalyzed cyanation protocol using NaCN.[41] Introducing the electron-rich aromatic group onto the vinyl nitrile is accomplished using a Rh-catalyzed 1,4-addition reaction developed by the Hayashi group, providing *trans*-β-aryl nitrile **25** in 69% yield (78% brsm).[42] The ester moiety is selectively reduced to the primary alcohol with Red-Al, leaving the nitrile intact (77%). The primary hydroxyl is oxidized to aldehyde **26** (89%), which is subsequently methylenated to alkene **27** (98%). In the presence of acid-labile functionalities such as
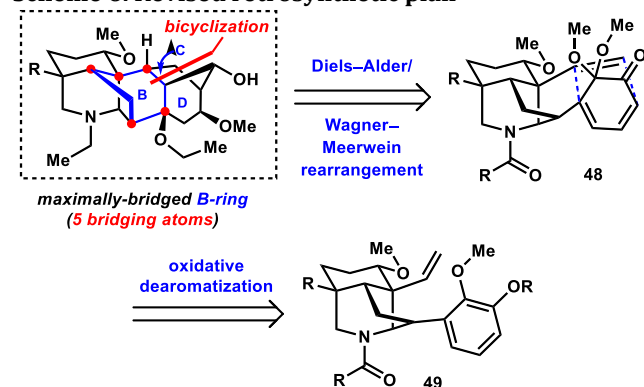
the silyl ether, hydration of the nitrile to afford primary amide **29** proceeds in 65–75% yield under anhydrous conditions employing Wilkinson's catalyst and acetaldoxime as the water-equivalent.[43] Hypervalent iodine-mediated Hofmann rearrangement of **29** in methanol solvent forms the corresponding methyl carbamate, which is then subjected to TBAF-mediated deprotection to reveal alcohol **30** in 94% yield over two steps. Successive activation of the alcohol as the mesylate and treatment with KH in DMF results in cyclization to piperidine **31** (88% yield over two steps), which served as our substrate for photocycloaddition studies.

Irradiation of a solution of vinyl arene **31** in C$_6$D$_6$ with 254 nm UV light results in the formation of diastereomeric [2+2]-cycloadducts **32** and **33** (Scheme 5a) via *ortho*-π-arene photocycloaddition. Using 310 nm UV light gives a similar outcome by ^{1}H NMR analysis. Attempts to isolate these cycloadducts by silica gel chromatography resulted in their decomposition to a mixture of hydrolyzed products. However, reconstituting this mixture of **32** and **33** in methanol with *p*-TsOH fully converts the bis-enol ether intermediates to an isomeric mixture of hexacyclic, vinylogous esters **34**, **35**, and **36** in 12%, 28%, and 8% yields,
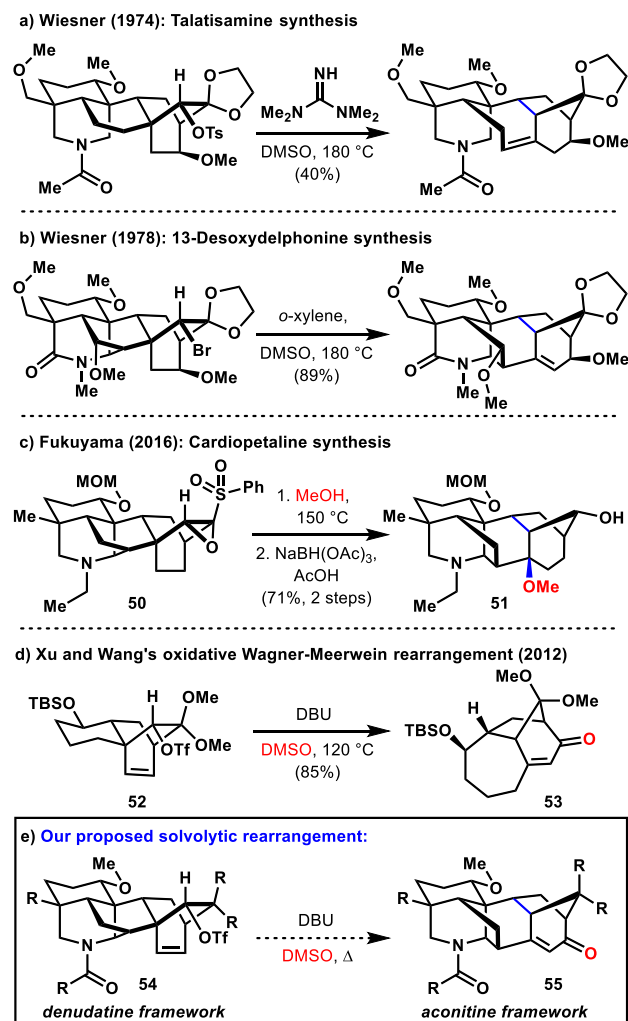
respectively. These cycloadducts were unambiguously characterized by single-crystal X-ray crystallography. Products arising from formation of exciplex **37** and the desired (3+2) *meta*-π-arene photocycloaddition pathway were not observed (e.g., **38**). UV irradiation in other non-polar solvents such as cyclohexane and toluene at room temperature or 4 °C has minimal effect on reactivity, and the use of methanol as solvent partially facilitates hydrolysis of photocycloadducts **32** and **33**. The lack of (3+2) reactivity is likely due to the developing strain that is imposed by tethering the alkene *meta* to the methoxy-directing groups, a substitution pattern that has not been demonstrated to undergo *meta*-π-arene photocycloaddition.[35] To help alleviate strain, bicyclic vinyl arenes **27** and **39** (precursors to alcohol **30**) were subjected to 254 nm UV irradiation (Scheme 5b). However, reducing strain by not having the piperidine ring in place results in no reactivity, likely due to the system being unable to adopt an energetically-accessible, reactive conformation. Based on similar reasoning, a less constrained vinyl arene (**40**) lacking the C7–C17 bond was prepared and irradiated with 254 nm UV light (Scheme 5c). While reactive, this substrate gives rise to a complex mixture of products that could not be easily purified. To test whether the lack of (3+2) reactivity could be due to a high barrier in forming a strained 6-membered B-ring, we designed substrate **41** where the alkene is tethered *ortho* to the methoxy-group (Scheme 5d). In this case, if a (3+2) photocycloaddition were to occur through exciplex **42** and diradical **43**, a more favorable 5-membered B-ring (highlighted in red) would form. This hypothesis proved correct, providing (3+2) cycloadduct **44** as the major product in 44% yield. The [2+2] cycloaddition pathway is also operative to a small extent, affording cyclobutene-bearing **47** in 16% yield. This product differs from the previously observed *ortho*-photocycloaddition reactions (*cf.* Scheme 5a) in that cyclobutene intermediate **45** bearing a tertiary methoxy group formed from the initial photochemical [2+2]-cycloaddition, undergoes spontaneous 6π-electrocyclic ring opening to cyclooctatriene **46**, followed by a final photochemical 4π-electrocyclic ring closing process to arrive at **47**.[44] These products, however, could not be easily advanced to the target natural products.

A bioinspired Wagner–Meerwein rearrangement approach to the BCD ring system. An alternative bicyclization disconnection that still retrosynthetically cleaves the maximally-bridged B-ring of the aconitine-type frame-

Scheme 6. Revised retrosynthetic plan

maximally-bridged B-ring
(5 bridging atoms)

Scheme 7. Wagner–Meerwein approaches to the [3.2.1]-bicyclic motif (BCD ring system)

a) Wiesner (1974): Talatisamine synthesis

b) Wiesner (1978): 13-Desoxydelphonine synthesis

c) Fukuyama (2016): Cardiopetaline synthesis

d) Xu and Wang's oxidative Wagner-Meerwein rearrangement (2012)

e) Our proposed solvolytic rearrangement:

denudatine framework   *aconitine framework*

work involves a [4+2]-cycloaddition between the alkene and the arene system following oxidative dearomatization (Scheme 6). The product will contain a bicyclo[2.2.2]-octane system characteristic of the denudatine-type molecules that will need to be rearranged to give the bicyclo[3.2.1] CD-ring system. Since nature employs such an isomerization in the biosynthesis of numerous diterpenes by rearranging the diterpene skeleton of denudatine alkaloids to that of the aconite skeleton,[45–48] we reasoned that this approach could offer promising opportunities for developing a divergent synthesis. In fact, Wagner–Meerwein-type rearrangement of a bicyclo[2.2.2]octane to the corresponding bicyclo[3.2.1]octane was first reported in 1949[49,50] by Doering et al. and successfully applied to early syntheses of the diterpenoid alkaloids talatisamine[51] and 13-desoxydelphonine[52] by Wiesner and coworkers (Schemes 7a and 7b). More recently, Fukuyama and coworkers disclosed an unusual solvolytic rearrangement of sulfonyloxirane **50**, followed by reduction of the resultant ketone to alcohol **51** (Scheme 7c). We were particularly interested in implementing a process reported by Xu and Wang in 2012,[53] in which an oxidative Wagner–Meerwein-type rearrangement on the

**Scheme 8. Formation of the key hexacyclic intermediate containing [2.2.2]-bicycle**
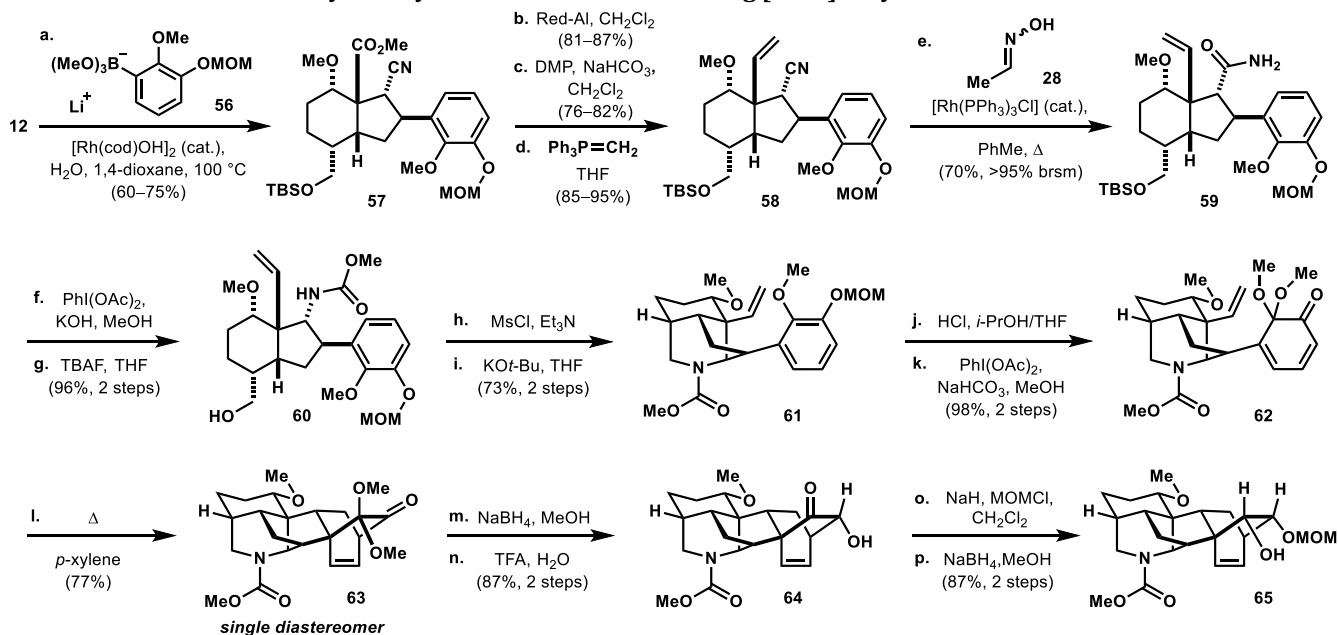
^{a} Reaction conditions: (a) **56** (prepared from the corresponding ArBr), n-BuLi, Et$_2$O, −78 to 23 °C; then B(OMe)$_3$, −40 °C; then **12**, [Rh(cod)OH]$_2$ (cat.), H$_2$O, 1,4-dioxane, 100 °C, 60−75%; (b) Red-Al, CH$_2$Cl$_2$, 0−23 °C, 81−87%; (c) DMP, NaHCO$_3$, CH$_2$Cl$_2$, 76−82%; (d) PPh$_3$MeBr, LiHMDS, THF, 70 °C; then aldehyde, 0−23 °C, 85−95%; (e) **28**, [Rh(PPh$_3$)$_3$Cl] (cat.), PhMe, 130 °C, 70% (>95% brsm); (f) PhI(OAc)$_2$, KOH, MeOH; (g) TBAF, THF, 23 °C, 96% over 2 steps; (h) MsCl, Et$_3$N, CH$_2$Cl$_2$; (i) KOt-Bu, THF, 73% over two steps; (j) HCl, i-PrOH/THF; (k) PhI(OAc)$_2$, NaHCO$_3$, MeOH, 98% over two steps; (l) p-xylene, 150 °C, 77%; (m) NaBH$_4$, MeOH; (n) TFA, H$_2$O, 87% over two steps; (o) NaH, MOMCl, CH$_2$Cl$_2$; (p) NaBH$_4$, MeOH, 87% over 2 steps.

bicyclo[2.2.2]octene system of **52** furnishes the bicyclo[3.2.1] system of **53** with concomitant introduction of a new oxygen atom (Scheme 7d). The alkene group in **53** also presents additional opportunities for functionalization, which we envisioned to be useful for generating diversity when planning natural and unnatural product synthesis. We thus targeted hexacycle **54**, which exhibits the denudatine framework, with the intention of rearranging it to **55**, which exhibits the aconitine framework, via an oxidative Wagner–Meerwein rearrangement (Scheme 7e).

The synthesis of the denudatine framework commences with the 1,4-arylation of vinyl nitrile **12** using aryl boronate ester **56** to form β-aryl nitrile **57** in 60−75% yields (Scheme 8). Similar to the sequence illustrated in Scheme 4, selective reduction of the methyl ester to its corresponding primary alcohol (81−87% yields), followed by oxidation (76−82% yields) and Wittig olefination (85−95% yields) provides alkene **58**. Subjecting **58** to Rh-catalyzed nitrile hydration gives the desired primary amide (**59**) in 70% yield, with the remainder of the mass balance accounted for by unreacted starting material that can be resubjected to the same reaction conditions. The primary amide is effectively converted to its corresponding methyl carbamate by treatment with PhI(OAc)$_2$ in methanol and the primary alcohol deprotected with TBAF to yield **60** in 96% over the two steps. Mesylation of the alcohol and cyclization of the piperidine ring occurs by reacting **60** with MsCl/Et$_3$N and KOt-Bu, respectively, to give tricycle **61** in 73% yield over the two steps. Subsequent cleavage of the MOM protecting group with HCl and oxidative dearomatization with PhI(OAc)$_2$ in methanol furnishes dienone **62**, the immediate precursor to intramolecular Diels–Alder cycloaddition, in 98% yield over two steps. Heating a solution of **62** in p-xylene to 150 °C in a sealed flask induces

the intramolecular [4+2]-cycloaddition to provide the desired hexacycle (**63**) as a single diastereomer in 77% yield. Reduction of the ketone carbonyl of **63** occurs exclusively from the more sterically-encumbered β-face (see the SI), which is then followed by acid-catalyzed cleavage of the dimethyl ketal to reveal α-hydroxy ketone **64** in 87% yield. This secondary hydroxy-group is masked as the MOM-ether by treatment with NaH and MOMCl, and a NaBH$_4$-mediated reduction of the remaining carbonyl group again occurs exclusively from the β-face, generating α-disposed alcohol **65** in 87% yield over two steps. Xu and Wang observed a similar β-selective NaBH$_4$ reduction in their synthesis of model substrate **52** (see Scheme 7d); however, they stated that a rationalization for the observed selectivity could not be provided. We postulate that the exclusive approach from the β-face of the molecule arises from a torsional steering effect: reduction from the seemingly less-hindered α-face would give rise to an unfavorable eclipsing interaction in the transition state whereas reduction from the seemingly more-hindered β-face would lead directly to an energetically-favorable transition state with a staggered conformation (Scheme 9).

Scheme 9. Torsional steering controls NaBH$_4$ reduction
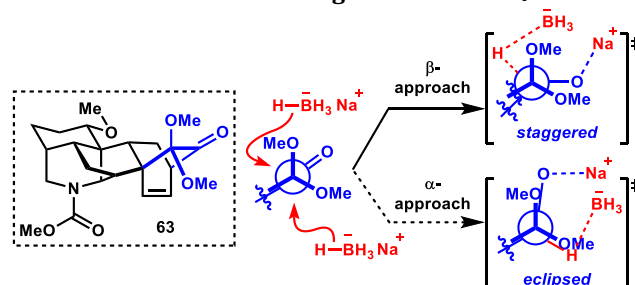
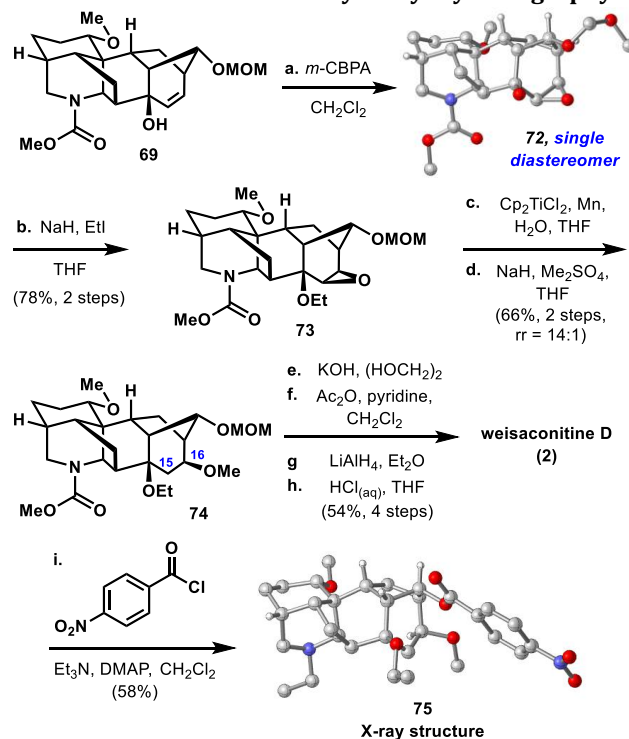**Scheme 10. Wagner–Meerwein rearrangement and possible mechanisms**
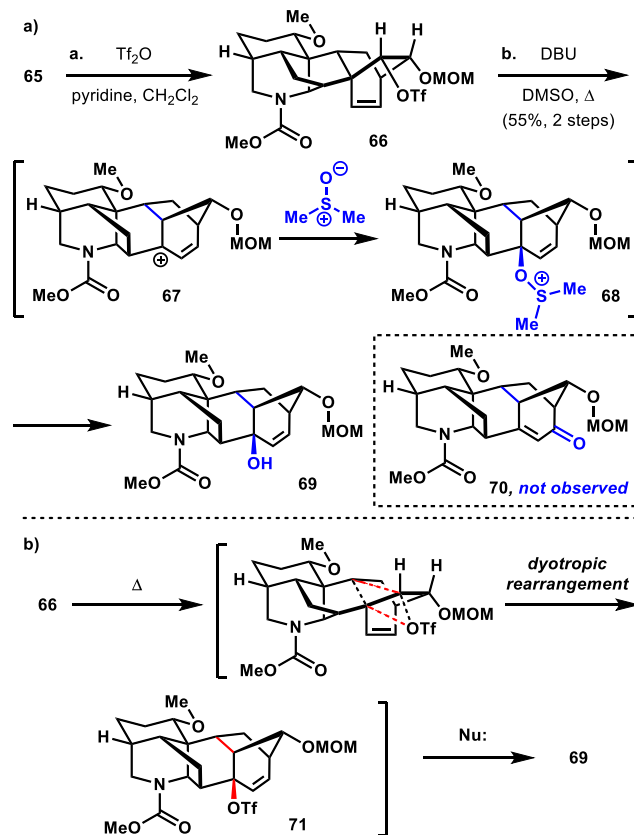
a Reaction conditions: (a) Tf$_2$O, pyridine, CH$_2$Cl$_2$, −78 to 23 °C; (b) DBU, DMSO, 120 °C, 55% over two steps. DBU = 1,8-diazabicyclo[5.4.0]undec-7-ene.

Scheme 11. Completion of weisaconitine D and confirmation of chemical structure by X-ray crystallography

a Reaction conditions: (a) *m*-CPBA, CH$_2$Cl$_2$, 0–23 °C; (b) NaH, EtI, THF, 0–40 °C, 78% over two steps; (c) Cp$_2$TiCl$_2$, Mn, H$_2$O, THF, 23 °C; (d) NaH, Me$_2$SO$_4$, THF, 66% over 2 steps, rr = 14:1; (e) KOH$_{(aq)}$, (HOCH$_2$)$_2$; (f) Ac$_2$O, pyridine, CH$_2$Cl$_2$, 0–23 °C; (g) LiAlH$_4$, Et$_2$O, 0–40 °C; (h) 2 N HCl$_{(aq)}$, THF, 54% over four steps; (i) 4-O$_2$NC$_6$H$_4$COCl, Et$_3$N, DMAP, CH$_2$Cl$_2$, 0–23 °C, 58%.

Activating alcohol **65** with triflic anhydride, and then heating the newly formed triflate (**66**) in a mixture of DBU and DMSO resulted in the formation of allylic alcohol **69** as the only observable product (Scheme 10). Enone **70**, which was anticipated on the basis of the precedent by Xu and Wang, was not formed to any appreciable extent. One possible pathway involves a thermally-induced 1,2-alkyl shift leading to the formation of tertiary, allylic carbocation **67**, which is trapped by the DMSO solvent, and ultimately affords allylic alcohol **69** through an elimination pathway (Scheme 10a). In contrast, enone **70** would arise through an S$_N$2' addition of DMSO to the less hindered position of allylic carbocation **67** followed by oxidation of the allylic hydroxyl. Presumably, the strain imposed by the alkene group of the enone precludes the formation of **70**.[54] Alternatively, a dyotropic rearrangement[55] involving simultaneous, concerted migration of the alkyl and triflate groups through the intermediacy of allylic triflate **71**, can be invoked to explain the observed selectivity for **69** (Scheme 10b).

Synthesis of C$_{18}$ weisaconitine D. Allylic alcohol **69**, although unanticipated, bears the desired bicyclo[3.2.1] octene system that can be advanced to weisaconitine D (**2**).[56] Alcohol **69** also possesses the framework of other C$_{18}$ and C$_{19}$ diterpenoid alkaloids such as the lappaconitines, ranaconitines, and aconitines.[57] Epoxidation of **69** yields epoxy alcohol **72** as a single diastereomer (Scheme 11). X-ray crystallographic analysis of this intermediate provided

unambiguous confirmation of its structure and stereochemistry. The alcohol group was alkylated to give epoxy ether **73** in 78% yield over two steps. A titanium(III)-mediated epoxide ring opening using water as the hydrogen atom source[58] occurs regioselectively, and the hydroxyl obtained in this manner was methylated in 66% yield over two steps with an isomeric ratio of 14:1 (the minor isomer has the methoxy group at C15, not shown). To introduce the *N*-ethyl substituent, the carbamate of **74** was first cleaved by base-mediated hydrolysis, and the unveiled piperidine nitrogen acetylated with Ac$_2$O and reduced with LiAlH$_4$. As discussed later, installing the ethyl group in a more direct fashion would not yield a more efficient synthesis (Scheme 15). A final deprotection with aqueous HCl cleaved the MOM-protecting group and accomplished the first synthesis of weisaconitine D (54% yield over the last four steps). Derivatizing **2** to *p*-nitrobenzoylated **75** allowed us to acquire a single crystal X-ray structure to support the characterization of the natural product.

Synthesis of C$_{19}$ liljestrandinine.[59] All of the C$_{19}$- and C$_{20}$-diterpenoid alkaloids contain an additional carbon atom (C18) at C4 with respect to the C$_{18}$ natural products (see Figure 1). Using an intermediate (**60**, Scheme 8) from the synthesis of weisaconitine D (**2**), we initially sought to introduce this one-carbon unit through an enolate alkylation reaction (Scheme 12a). Thus, alcohol **60** was oxidized to aldehyde **76** in 95% yield under typical Swern conditions. We expected that exposure of **76** to base and a

Scheme 12. α-Alkylation generates only the undesired diastereomer

a)
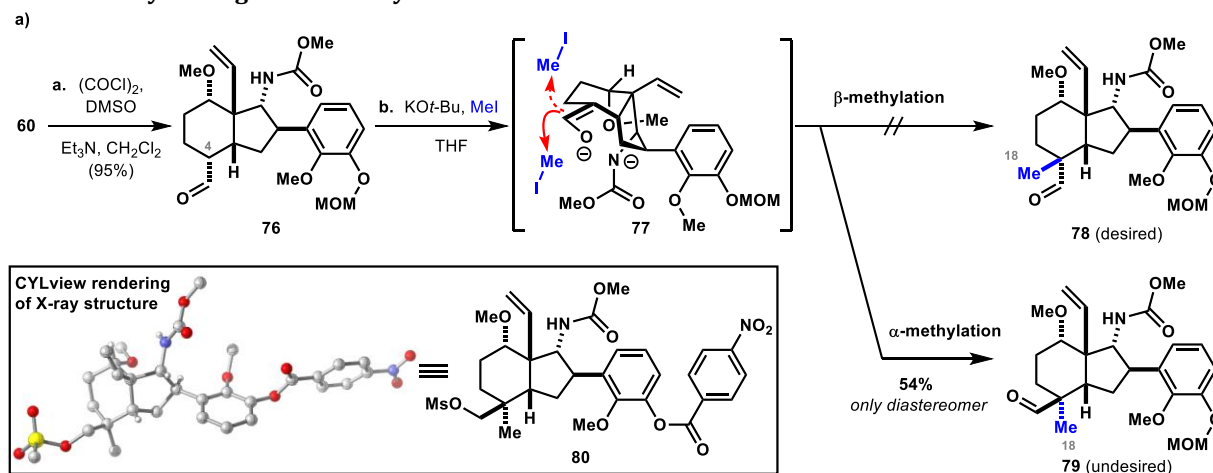
b) Two views of dianion 77 optimized in the gas phase at the B3LYP/6-31+G(d,p) level of theory
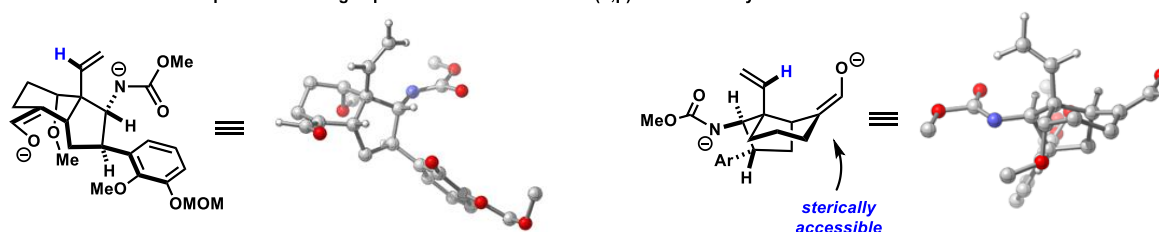
a Reaction conditions: (a) (COCl)₂, Et₃N, CH₂Cl₂, −78 to 23 °C, 95%; (b) KO*t*-Bu, THF, 0 °C, then MeI, 54% **79**.

methylating agent would effect α-alkylation from the convex face of the bicycle. Treating **76** with excess KO*t*-Bu leads to formation of bicyclic enolate **77** with accompanying deprotonation of the methyl carbamate. However, reacting this enolate with iodomethane did not result in the desired alkylation from the convex face to give β-methyl aldehyde **78**, but instead alkylation occurred exclusively from the concave face of the bicycle to yield α-methyl aldehyde **79** in 54% yield. The stereochemistry of α-**79** was confirmed by its conversion to mesylate **80** and acquiring single crystal X-ray diffraction data. Unfortunately, the aldehyde of **79** is not correctly disposed for cyclization to yield the requisite piperidine structure. To gain insight into the observed alkylation selectivity, we modeled the intermediate (**77**) arising from the double deprotonation of aldehyde **76** by DFT at the B3LYP/6-31+G(d,p) level of theory (Scheme 12b). In the two views of the minimized structure, the vinylic proton (shown in blue) protrudes directly over the reactive p-orbital of the enolate, effectively shielding approach of the methyl electrophile from the convex face. In contrast, approach of the electrophile from the concave face is relatively unhindered, providing a rationale for the exclusive α-selectivity that is observed.

On the basis of this analysis, any type of electrophile should approach the enolate from the undesired concave face. Inspired by the precedent of Wiesner, transforming aldehyde **76** to diol **81** using an aldol-Cannizzaro reaction,[60] which we accomplished in 97% yield, obviates the need for a diastereoselective alkylation (Scheme 13). Attempts at selective deoxygenation directly from diol **81** using Morandi's protocol (Ph₂SiH₂/Et₃SiH and catalytic B(C₆F₅)₃)[61] or through a more traditional stannane-mediated deoxygenation[62] of thiocarbonate **83** gave com-

plex mixtures of products. In these reactions, the desired mono-deoxygenated products **82** and **84** were not formed in significant amounts. We next sought to synthesize bis-

Scheme 13. Alternative attempts at installing the C₄-methyl group
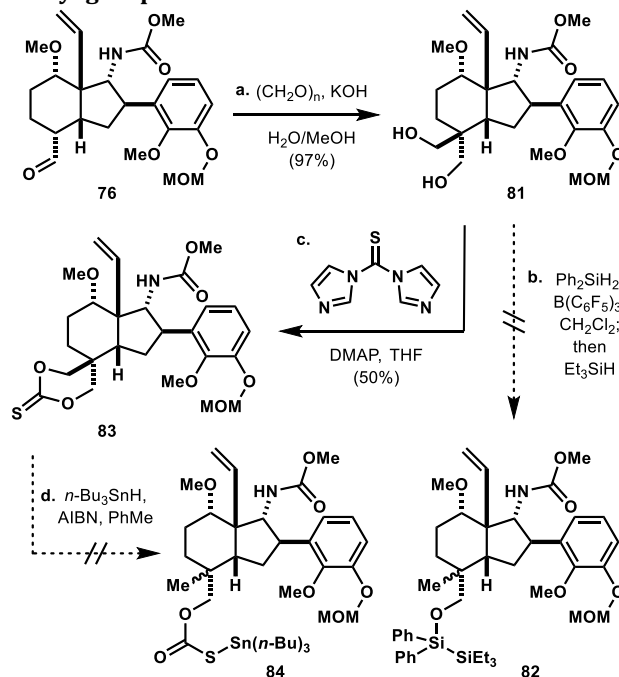
a Reaction conditions: (a) (CH₂O)ₙ, KOH, H₂O/MeOH, 97%; (b) B(C₆F₅)₃ (cat.), Ph₂SiH₂, CH₂Cl₂, then Et₃SiH; (c) thiocarbonyldiimidazole, DMAP, THF, 23–60 °C, 50%; (d) *n*-Bu₃SnH, AIBN, PhMe. DMAP = 4-dimethylamino-pyridine; AIBN = azobisisobutyronitrile

Scheme 14. Synthesis of C19-diterpenoid alkaloid liljestrandinine
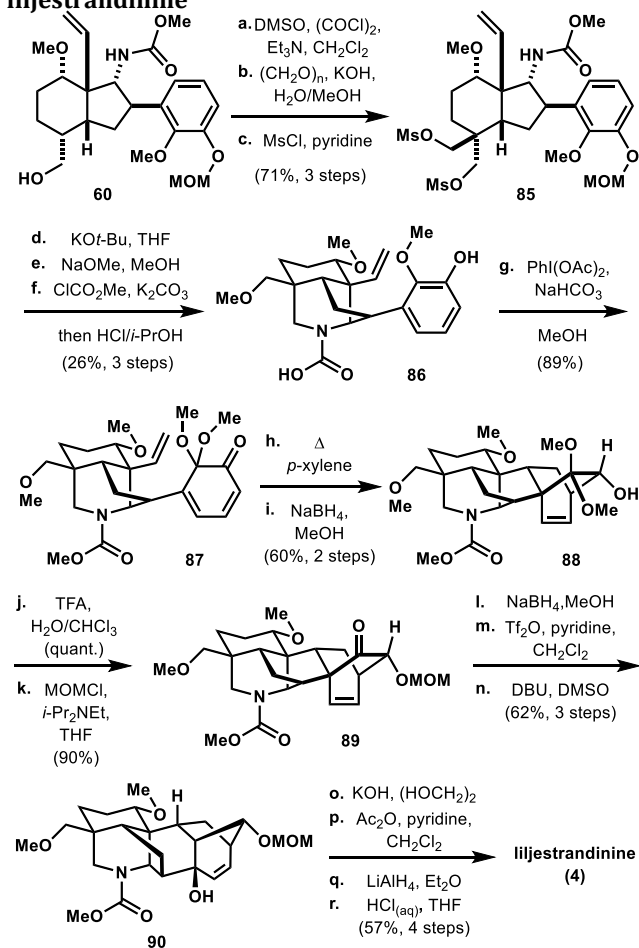
a Reaction conditions: (a) DMSO, (COCl)₂, Et₃N, CH₂Cl₂, −78 to 23 °C; (b) (CH₂O)ₙ, KOH, H₂O/MeOH, 23 °C; (c) MsCl, pyridine, 0–23 °C, 71% over three steps; (d) KOt-Bu, THF, 50 °C; (e) 0.5 M NaOMe in MeOH, 120 °C; (f) ClCO₂Me, K₂CO₃, acetone, reflux; then 2 N HCl, i-PrOH, 23 °C, 26% over three steps; (g) PhI(OAc)₂, NaHCO₃, MeOH, 0 °C, 89%; (h) p-xylene, 150 °C; (i) NaBH₄, MeOH, 0–23 °C, 60% over two steps; (j) TFA, H₂O/CHCl₃, 0 °C, quant.; (k) MOMCl, i-Pr₂NEt, THF, 0–23 °C, 90%; (l) NaBH₄, MeOH, 0 °C; (m) Tf₂O, pyridine, CH₂Cl₂, −78 to 23 °C; (n) DBU, DMSO, 120 °C, 62% over three steps; (o) KOH(aq), (HOCH₂)₂, 100 °C; (p) Ac₂O, pyridine, CH₂Cl₂, 0–23 °C; (q) LiAlH₄, Et₂O, CH₂Cl₂, 0–40 °C; (r) 12 N HCl(aq), THF, 23 °C, 57% over four steps. TFA = trifluoroacetic acid; DBU = 1,8-diazabicyclo[5.4.0]undec-7-ene.

mesylate **85**. This was achieved through an optimized three-step sequence from alcohol **60** in 71% overall yield, involving Swern oxidation, an aldol-Cannizzaro reaction, and mesylation (Scheme 14). We reasoned that the carbamate nucleophile should react selectively with the mesylate on the same face. Thus, addition of KOt-Bu to **85** results in displacement of the α-mesylate to form the piperidine ring and ensuing addition of NaOMe displaces the remaining mesylate to form the methoxymethyl group. However, these basic conditions also led to undesired cleavage of the N-carbamoyl group, which was reintroduced by treating the crude mixture with methyl chloroformate. An acidic workup procedure ultimately yields tricycle **86** with the free phenolic group in 26% yield over the three steps (see Table 1 for an optimization of this process and its application to the syntheses of the C₂₀ natural products). Conversion of guaiacol derivative **86** to dienone **87** with hypervalent iodine occurs smoothly in 89% yield and sets the stage

for an intramolecular Diels–Alder reaction. Heating to 150 °C effectively transforms **87** into the Diels–Alder cycloadduct, and its ketone carbonyl is reduced stereoselectively with NaBH₄ to afford hexacyclic alcohol **88** in 60% yield over two steps. The ketal hydrolysis and MOM protection occurs in 90% yield over two steps. Similar to the protocol adopted for the synthesis of weisaconitine D (**2**, Scheme 8), the ketone group in **89** is stereoselectively reduced to the corresponding secondary alcohol from the desired β-face, and the resulting alcohol activated for skeletal rearrangement by triflation. Heating the resultant triflate with DBU and DMSO affords allylic alcohol **90**, which contains the desired aconitine core, in 62% yield over three steps. A final four-step sequence involving piperidine deprotection, N-acetylation, amide reduction, and MOM cleavage was executed in 57% yield to complete the first synthesis of liljestrandinine (**4**).

Synthesis of C20-diterpenoid alkaloids. In developing syntheses of weisaconitine D (**2**) and liljestrandinine (**4**), we prepared intermediates that possess the denudatine framework and solvolytically rearranged these scaffolds to molecules that have the aconitine core structure. We thus aimed to take advantage of these intermediates to access denudatine-type natural products. Like liljestrandinine, the C20-diterpenoid alkaloids contain a carbon atom at C4, but in the form of a methyl group (C18, see Figure 1). To install this carbon, we surmised that a sequence similar to that used to install the methoxymethyl group of liljestrandinine (Scheme 14, steps a-f) would be most effective. However, the low yield (26%) associated with forming the piperidine ring and transforming the second mesylate needed to be improved in order for this sequence of reactions to be truly useful in synthesizing any of the C20-alkaloids.

The formation of the piperidine E-ring was thus reinvestigated. In contrast to the mesylation and subsequent KOt-Bu-mediated cyclization of alcohol **60** (Scheme 8), which occurs in good yield, the analogous KOt-Bu-mediated cyclization of bis-mesylate **85** occurs in a low 30% yield, with the majority of the mass balance accounted for by free amine **94**, which is isolated in 39% yield (Table 1, entry 1). A similar cleavage of carbamates using KOt-Bu in THF has been reported in the literature.[63] By switching to KH in THF, the isolated yield for piperidine **91** increases to 62%. Under these conditions, exocyclic alkene **92** and oxetane **93** are each produced in 8% yields, while the decarbamoylation side product **94** is formed in only trace quantities (LC-MS analysis; entry 2). As a consequence of the poor solubility of bis-mesylate **85** in THF, elevated temperatures between 50–60 °C are necessary to facilitate dissolution of the substrate and achieve reactivity. Presumably, the high temperatures are responsible for some of the undesired side reactions that were observed. Performing the same reaction with DMF as the solvent at room temperature results in exclusive formation of desired piperidine **91** in 83% yield (entry 3).

With robust conditions established for installing the piperidine moiety, we next turned our attention to transforming the methylene mesylate group in **91** to a methyl group (Scheme 15). Attempts to reduce **91** with lithium triethylborohydride[64] and the CuCl₂·2H₂O/Li/catalytic 4,4'-di-t-butylbiphenyl system[65] failed, returning only unreacted starting material. The lack of reactivity is presumably

Table 1. Optimization of E-ring piperidine formation

Entry	Conditions	91	92	93	94
1	KOt-Bu (3 equiv), THF, 50 °C	30%	0%	0%	39%
2	KH (1.6 equiv), THF, 55–60 °C	62%	8%	8%	trace
3	KH (1.6 equiv), DMF, rt	83%	0%	0%	0%

Scheme 15. Synthesis of cochlearenine, *N*-ethyl-1α-hydroxy-17-veratroyldictyzine, and paniculamine

[a] Reagents and conditions: (a) NaI, Zn⁰, DME, 105 °C; (b) HCl, THF/*i*-PrOH, 23 °C; (c) PhI(OAc)₂, NaHCO₃, MeOH, 23 °C, 61% over three steps; (d) *p*-xylene, 150 °C, 80-87%; (e) Me₂S(O)=CH₂, THF/DMSO, 0-21 °C, 85%; (f) Ph₃P=CH₂ (from Ph₃PMeBr, LiHMDS, 70 °C), 0-40 °C, then 1 M HCl(aq), 96%; (g) Ph₃CO₂Li (from Ph₃CO₂H, MeLi), THF, 0-40 °C, 57% (64% brsm); (h) HBr, AcOH, microwave (110 °C), 50 min, then 2 M NaOH(aq); (i) Ac₂O, pyridine, CH₂Cl₂, 0-23 °C, ~5% **100** + 28% **101** + 22% **102** + 29% **103** over two steps (84% combined yield); (j) KOAc, AcOH, 120 °C; (k) H₂ (100 psi), Pd/C (cat.), MeOH, 23 °C; (l) LiAlH₄, THF, 0-23 °C, three steps (63% from **102**, 77% from **103**); (m) H₂O₂, MeOH/H₂O, 60 °C, 50%; (n) veratroyl chloride, polymer-supported DMAP, CH₂Cl₂, 0-23 °C, 25% (34% brsm); (o) TFA, CDCl₃, quant. DMAP = dimethylaminopyridine; TFA = trifluoroacetic acid.

due to the steric congestion at the neopentyl mesylate site. The desired reduction, however, is accomplished using a combination of NaI and Zn and holding the reacting mixture at reflux in DME. Successive acidic cleavage of the MOM protecting group and oxidative dearomatization generates masked *o*-benzo-quinone **95** (61% yield over three steps) which was then heated to 150 °C in *p*-xylene to furnish Diels–Alder cycloadduct **96** (80–87% yields). To complete the C_{20} denudatine core, a final one-carbon unit needed to be delivered to the ketone group of **96**. We opted to use the Corey–Chaykovsky reagent,[66] which would provide an epoxide that can be conveniently elaborated to the target natural products. Contrary to the stereoselectivity observed for nucleophilic addition with $NaBH_4$ (Scheme 9) which we postulate to be governed by torsional steering and results in nucleophilic approach from the β-face, dimethylsulfoxonium ylide approaches ketone **96** from the opposite, less sterically-demanding α-face to yield epoxide **97** as a single, albeit the undesired, diastereomer in 85% yield. To obtain the desired epoxide diastereomer that can be advanced to the C_{20}-targets, **96** was subjected to a Wittig olefination, which after an acidic workup produces enone **98** in 96% yield. We hypothesized that delivery of an oxygen atom can occur from the α-face provided a sufficiently large oxidant is used. As postulated, a Weitz-Scheffer epoxidation[67] with trityl hydroperoxide forges the desired α-epoxide (**99**) in 57% yield (64% brsm) as the sole diastereomer. To cleave the methyl ether and methyl carbamate, **99** is heated in a mixture of HBr in AcOH under microwave conditions, and then basified with aqueous NaOH.[68] Ensuing treatment with Ac_2O and pyridine acetylates the free amine, and leads to the isolation of elimination product **100** (~5% yield), fragmentation product **101** (28% yield), and the desired demethylated products **102** and **103** (51% combined yield). LC-MS analyses suggest that the 1-acetoxy group of **103** is introduced during the dealkylation step with HBr in AcOH and not during the subsequent acetylation step with Ac_2O. Epoxide ring-opening was effected in the presence of KOAc in AcOH, affording α-hydroxyketone **104**. This was followed by hydrogenation of the strained alkene using Pd/C and global reduction with $LiAlH_4$ in 63–77% yield over three steps, which accomplished the first synthesis of cochlearenine (**6**).

We found density functional theory (DFT) to be critical in confirming the structures of the natural products.[69] Cochlearenine (**6**) has been isolated and characterized twice in the literature, albeit with significant discrepancies between the two sets of data.[70,71] The spectroscopic data obtained by us for synthetic **6** are consistent with those reported by Wada et al. apart from one ^{13}C signal, raising the concern that the C15-epimer of the natural product might have formed during the global reduction step (Scheme 15, step l). We thus computed the ^1H and ^{13}C NMR data for both cochlearenine (**6**) and its C15-epimer, and found that our experimental data closely agree with the computed data for the natural product with a computed mean absolute deviation (CMAD) of 0.14 ppm for the ^1H NMR data and 1.5 ppm for the ^{13}C NMR data (see SI). This analysis also allowed us to discount the possibility of having formed the C15-epimer, which exhibits larger CMADs of 0.21 ppm and 2.9 ppm for the ^1H NMR and ^{13}C NMR data,
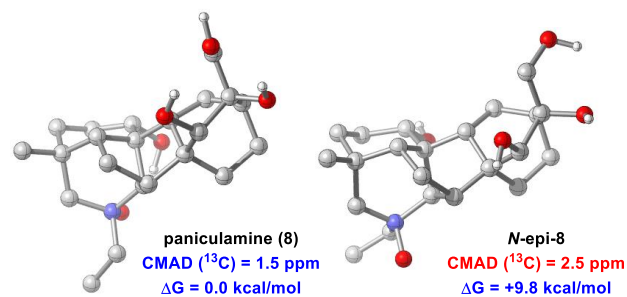

Figure 2. Optimized geometries for paniculamine (**8**) and its epimer computed at the M06-2X/6-31+G(d,p)/IEFPCM (H_2O) level of theory.

respectively, compared to the synthetic material.

The primary hydroxyl (C17 position) of cochlearenine (**6**) is veratroylated by exposure to veratroyl chloride and polymer-supported DMAP to give **7** in 25% yield (34% brsm). In this case, the acquired spectroscopic data for the neutral amine bears no resemblance to that reported in the isolation disclosure.[72] An attempt to acidify **7** with anhydrous HCl in diethyl ether resulted in a species with a ^1H NMR spectrum that exhibits broad signals differing significantly from those reported by Díaz et al. However, titrating **7** with trifluoroacetic acid distinctly converts the neutral species to its protonated state, **7·TFA** (see SI), the spectroscopic data of which is fully consistent with the reported data. This observation also supports our assignment of cochlearenine (**6**).

Finally, paniculamine (**8**) was prepared as a single diastereomer in 50% yield by treating **6** with aqueous H_2O_2. Because the ^1H NMR data for **8** is only partially reported in the isolation study, and the ^{13}C NMR data not reported at all,[73] we used DFT to confirm the identity of our synthetic material. The computed ^1H and ^{13}C spectra for **8** matches closely our experimental data with CMADs of 0.23 ppm and 1.5 ppm, respectively. In contrast, larger discrepancies with CMADs of 0.27 ppm for the ^1H NMR data and 2.5 ppm for the ^{13}C NMR data were found for **N-epi-8** compared to those of the synthesized compound. Altogether, the results suggest that the synthesized material is consistent with the structure of **8**. The natural product is also found to be 9.8 kcal/mol lower in energy than its *N*-epimer, presumably in large part due to a favorable enthalpic interaction between the oxygen of the *N*-oxide and the 1-hydroxy group (Figure 2). Thus, the oxidation to form **8** is likely both thermodynamically and kinetically favored, with the 1-hydroxy group directing oxidation from the back face of the piperidine ring.

Early installation of an *N*-ethyl substituent. Because all of the natural products that we have targeted bear an *N*-ethyl substituent, the use of the *N*-carbamate as a protecting group does not provide the most direct approach since it requires three additional steps (decarbamoylation, acetylation, amide reduction) to transform it into the *N*-ethyl group. In addition, hydrolysis of carbamates **74** (Scheme 11, step e) and **90** (Scheme 14, step o) is slow and requires harsh conditions (4 M KOH, 100 °C, 60–120 h). We thus explored the possibility of introducing the *N*-ethyl substituent early on. Instead of submitting primary amide **59** to Hofmann rearrangement conditions in MeOH (Scheme 8), performing the reaction in CH_3CN solvent forms the isocy-

Scheme 16. Studying the feasibility of protecting the E-ring piperidine with an acetyl group
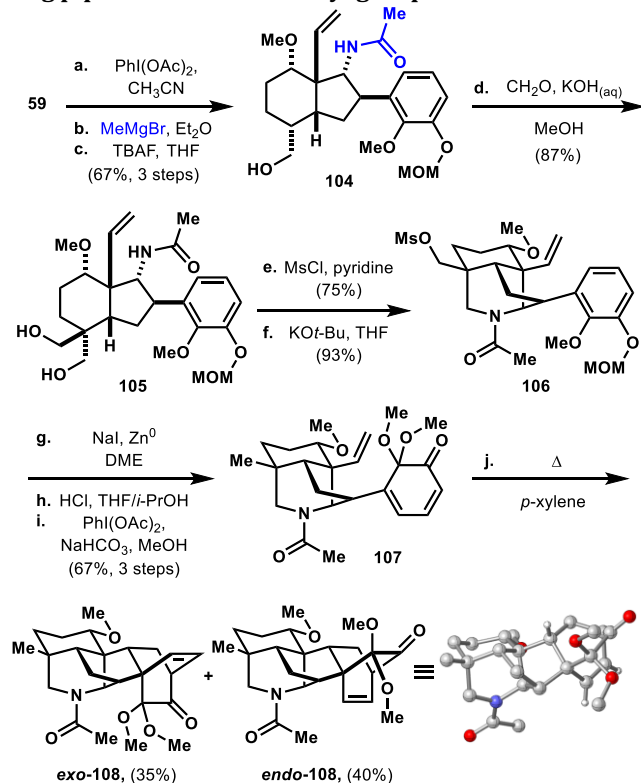
a Reaction conditions: (a) PhI(OAc)$_2$, CH$_3$CN, 0-23 °C; (b) MeMgBr, Et$_2$O, 0 °C; (c) TBAF, THF, 23 °C, 67% over three steps; (d) formalin, KOH$_{(aq)}$, MeOH, 23 °C, 87%; (e) MsCl, pyridine, 0–23 °C, 75%; (f) KO*t*-Bu, THF, 50 °C, 93%; (g) NaI, Zn^0, DME, 105 °C; (h) HCl$_{(aq)}$, THF/*i*-PrOH, 23 °C; (i) PhI(OAc)$_2$, NaHCO$_3$, 23 °C, MeOH, 67% over three steps); (j) *p*-xylene, 150 °C, 35% *exo*-**108** + 40% *endo*-**108**.

anate intermediate that can be trapped with methyl magnesium bromide to form alcohol **104**. This material was advanced to masked *ortho*-benzoquinone **107**, the precursor for the intramolecular Diels–Alder cycloaddition, using the same sequence developed for the synthesis of denudatine natural products **6**−**8**.
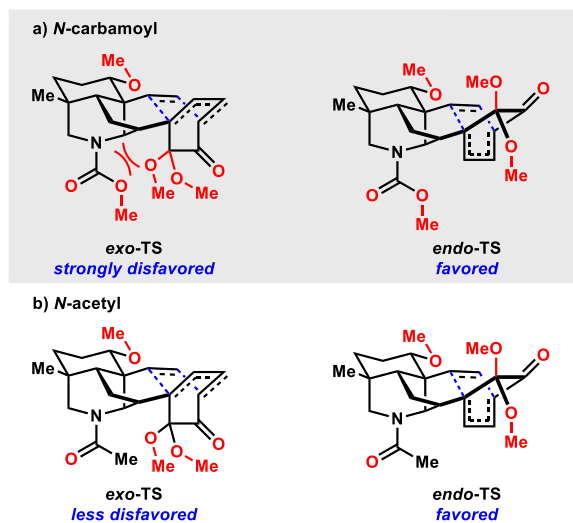

Figure 3. Proposed rationale for selective, intramolecular, Diels–Alder cycloaddition.

Surprisingly, the Diels–Alder reaction of **107** proceeds to yield a mixture of the undesired *exo*-**108** in 35% yield and the desired *endo*-**108** in 40% yield. This is in stark contrast to dienones **62** (Scheme 8), **87** (Scheme 14), and **95** (Scheme 16), which all bear carbamate protected piperidine structures, and undergo [4+2] cycloadditions with complete diastereocontrol for the desired *endo*-cycloadducts. A possible rationale for this observation is that the transition state leading to the *exo*-cycloadduct experiences substantial repulsive interactions between the oxygens of the carbamate and the *exo*-disposed dimethyl acetal (Figure 3a), an interaction that is absent in the *endo* transition state. In the case of the *N*-acetylated substrate (**107**), its *exo*-TS, while more sterically-encumbered, can orient the oxygen atom of the amide away from the dimethyl acetal and reduce some of the unfavorable repulsive interactions (Figure 3b). The *endo*-TS experiences less of the unfavorable interactions and is still formed as the major product. Regardless, the poor diastereoselectivity observed in this key transformation precluded the use of the *N*-acetyl group in the syntheses.

Enantioselective synthesis of *endo*-Diels–Alder cycloadduct 13. To synthesize weisaconitine D (**2**), liljestrandinine (**4**), cochlearenine (**6**), *N*-ethyl-1α-hydroxy-17-veratroyldictyzine (**7**), and paniculamine (**8**) in enantioenriched form, an initial enantioselective Diels–Alder cycloaddition to access *endo*-**13** is necessary. We initially sought to directly combine diene **21** and dienophile **22** enantioselectively by employing a cationic ruthenium(II) center coordinated to a chiral, tetradentate PNNP ligand, (1*S*,2*S*)-*N*,*N*′-bis[*o*-(diphenylphosphino)-benzylidene]cyclohexane-1,2-diamine,[74,75] or a copper(II) center ligated to a chiral bisoxazoline. When these complexes were applied as catalysts in our system, significant decomposition of diene **21** and minimal formation of the desired cycloadduct (**13**) were observed. The small

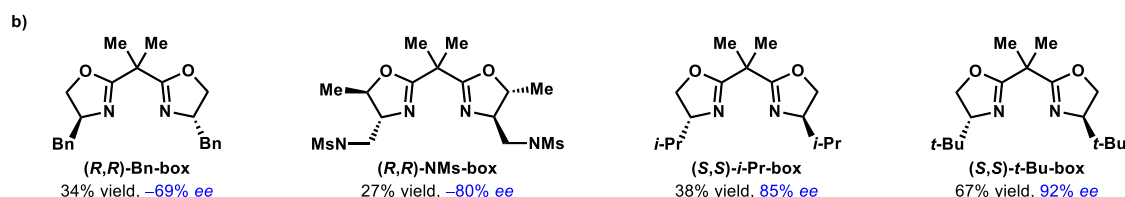**Table 2. Exploring reagents for selective imide methanolysis**

Entry	Reagent	Time (h)	R	114/115 ^{c}
1^a	NaOMe	4	TBS	2:1
2^b	AgOTf	48	TBS	no conv.
3^b	Cu(OTf)$_2$	2	TBS	2.9:1
4^b	Sn(OTf)$_2$	>48	H	2.5:1
5^b	Eu(OTf)$_3$	0.5	TBS	4.8:1
6^b	Sm(OTf)$_3$	0.5	TBS	3.8:1
7^b	Ga(OTf)$_3$	0.5	H	only **114**
8^b	Yb(OTf)$_3$	24	TBS	no conv.
9^b	**Bi(OTf)$_3$**	**5.5**	**H**	**1:10**

a 18 equiv NaOMe used, [**113**] = 0.1 M, 0−23 °C; *b* 10 mol % Lewis acid used, [**113**] = 0.1 M, 28 °C; *c* ratios determined by ^{1}H NMR analysis of the crude reaction mixtures.

Scheme 17. Development of an enantioselective Diels−Alder reaction

a)
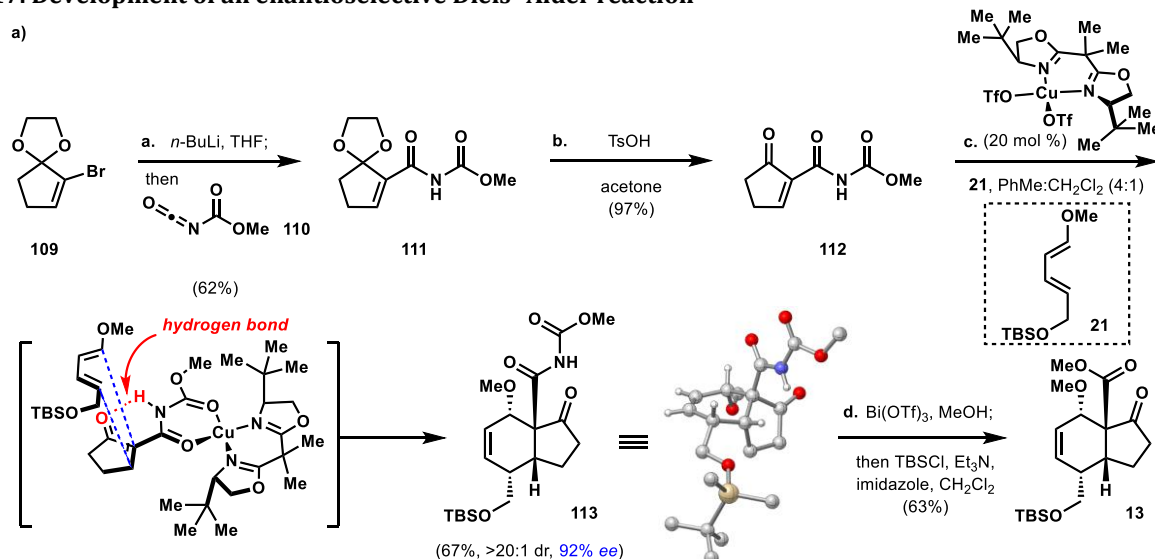
a Reagents and conditions: (a) *n*-BuLi, THF, −78 to −30 °C; then **110**, −78 °C, 62%; (b) TsOH, acetone, 0–23 °C, 97%; (c) [Cu-((*S*,*S*)-*t*-Bu-box)]OTf$_2$ (20 mol %), −20 °C, 67%, 92% ee; (d) Bi(OTf)$_3$ (35 mol %), MeOH, 23 °C; then TBSCl, Et$_3$N, imidazole, CH$_2$Cl$_2$, 63%

b)

(R,R)-Bn-box
34% yield, –69% *ee*

(R,R)-NMs-box
27% yield, –80% *ee*

(S,S)-i-Pr-box
38% yield, 85% *ee*

(S,S)-t-Bu-box
67% yield, 92% *ee*

a Reagents and conditions: **21** (2 equiv), **112** (1 equiv), [Cu-ligand]OTf$_2$ (20 mol %), PhMe/CH$_2$Cl$_2$ (4:1), −20 °C,40 h

amount of product obtained was of low *ee*, suggesting inadequate binding of the ketoester component of **22** to the catalyst. Inspired by the use of β-oxo imides in Cu-catalyzed Mukaiyama–Michael additions,[76] [4+2]-cycloadditions, and Hosomi–Sakurai reactions,[77] we hypothesized that incorporating the β-oxo imide motif into our dienophile could enhance binding of the dienophile to a Lewis-acid catalyst (relative to a β-ketoester) and facilitate Diels–Alder reactivity and selectivity. A scalable synthesis of β-oxo imide containing dienophile **112** was thus developed starting from vinyl bromide **109** (Scheme 17a). Lithium-halogen exchange, followed by nucleophilic addition to ethyl isocyanoformate **110** provides ketal **111** in 62% yield. Ketal hydrolysis using TsOH reveals β-oxo imide **112** in 97% yield. Upon subjecting a mixture of diene **21** and dienophile **112** to [Cu-((*S*,*S*)-*t*-Bu-box)](OTf)$_2$ catalysis, enantioselective [4+2]-cycloaddition proceeds to furnish *endo*-cycloadduct **113** in 67% yield (>20:1 dr) and 92% *ee*. Related copper catalysts modified with different BOX-ligands generally resulted in lower yields and *ee* (Scheme 17b).

To achieve the synthesis of enantioenriched **13**, selective methanolysis of the imide functionality of **113** at the "amide carbonyl" over the "carbamate carbonyl" is necessary. Methanolysis under standard conditions using NaOMe in MeOH resulted in a 2:1 mixture of products in favor of the undesired primary amide (**114**, Table 2, entry 1). We turned to Lewis acids with the intention of reversing the selectivity. AgOTf did not promote methanolysis even after extended reaction times (entry 2). Oxophilic di- and triva-

lent Lewis acids were more reactive. Cu(OTf)$_2$, Sn(OTf)$_2$, Eu(OTf)$_3$, and Sm(OTf)$_3$ were all capable of transforming **113** to mixtures of products favoring amide **114** over ester **115** in 2.5:1 to 4.8:1 selectivities (entries 3–6), with Sn(OTf)$_2$ simultaneously cleaving the silyl group. Ga(OTf)$_3$ completely favors the formation of **114** and results in deprotection of the alcohol (entry 7). While Yb(OTf)$_3$ is unreactive (entry 8), Bi(OTf)$_3$ desirably and effectively methanolyses the imide at the more hindered carbonyl to yield ester **115** with complete site selectivity (entry 9). We postulate that this mode of reactivity may result from coordination of bismuth to the ketone oxygen and the proximal "amide carbonyl," effectively activating it for nucleophilic substitution. Because this Lewis acid also cleaves the silyl group, a final step to re-silylate the alcohol group was required, producing the desired enantioenriched **13** in 63% yield. This enantioenriched bicycle can be used to access enantioenriched diterpenoid alkaloids.

CONCLUSION

Guided by network analysis, we accomplished a unified strategy to synthesize natural products belonging to each of the C$_{18}$-, C$_{19}$-, and C$_{20}$-families of diterpenoid alkaloids. Specifically, aconitine-type molecules weisaconitine D (**2**) and liljestrandinine (**4**) are synthesized in 30 and 29 steps, respectively, beginning from the initial Diels–Alder reaction between diene **21** and dienophile **22**. Denudatine-type cochlearenine (**6**), *N*-ethyl-1α-hydroxy-17-veratroyl-dictyzine (**7**) and paniculamine (**8**) are synthesized in 25, 26, and 26 steps, respectively, from hydrindenone **13**,

which is readily prepared on 30 g scale in a single pass. Advanced intermediate **60** is common to the synthesis of these natural products and is prepared on multigram scale per run. We have also developed a gram-scale enantioselective approach to **13** that should allow for the preparation of enantioenriched natural products. In doing so, we discovered a bismuth-catalyzed methanolysis of imide **113** that exclusively targets the more sterically-encumbered carbonyl. Motivated by the effectiveness of this network analysis approach, we have developed a freely accessible web-based program, that facilitates quick and accurate application of this concept by anyone in the synthetic community designing retrosyntheses.

ASSOCIATED CONTENT

Supporting Information.
This material is available free of charge via the Internet at http://pubs.acs.org.
    Crystallographic data for **34**
    Crystallographic data for **35**
    Crystallographic data for **36**
    Crystallographic data for **44**
    Crystallographic data for **47**
    Crystallographic data for *endo*-**108**
    Experimental procedures, characterization data for new compounds and the natural products, density functional theory energies and geometries

AUTHOR INFORMATION

Corresponding Author

*rsarpong@berkeley.edu

Present Addresses

† Theravance Biopharma US, Inc., 901 Gateway Boulevard, South San Francisco, CA 94080, USA
‡ The University of Chicago Law School, 1111 East 60th Street, Chicago, IL 60637, USA
§ World Wide Medicinal Chemistry, Groton Laboratories, Pfizer, Inc., Eastern Point Road, Groton, CT 06340, USA
¶ Department of Chemistry, Pfizer Pharmaceuticals, La Jolla Laboratories, 10770 Science Center Drive, La Jolla, CA 92121, USA
‖ Janssen Research & Development, LLC, 3210 Merryfield Row, San Diego, CA 92121-1126, USA

Notes

The authors declare no competing financial interest.

ACKNOWLEDGMENT

REFERENCES

(1) Atta-ur-Rahman; Choudhary, M. I. *Nat. Prod. Rep.* **1999**, *16*, 619.
(2) Wang, F.-P.; Chen, Q.-H.; Liu, X.-Y. *Nat. Prod. Rep.* **2010**, *27*, 529.
(3) Wang, X.-W.; Xie, H. *Drugs Future* **1999**, *24*, 877.
(4) Sun, J.; Peng, Y.; Wu, H.; Zhang, X.; Zhong, Y.; Xiao, Y.; Zhang, F.; Qi, H.; Shang, L.; Zhu, J.; Sun, Y.; Liu, K.; Liu, J.; A, J.; Ho, R. J. Y.; Wang, G. *Drug Metab. Dispos.* **2015**, *43*, 713.
(5) The C$_{18}$-Diterpenoid Alkaloids. In *The Alkaloids: Chemistry and Biology*; Cordell, G. A., Ed.; Academic Press: San Diego, 2009; Vol. 67, pp 1–78.
(6) Ameri, A. *Prog. Neurobiol.* **1998**, *56*, 211.
(7) Fujita, Y.; Terui, K.; Fujita, M.; Kakizaki, A.; Sato, N.; Oikawa, K.; Aoki, H.; Takahashi, K.; Endo, S. *J. Anal. Toxicol.* **2007**, *31*, 132.
(8) Stevens, M.; Peigneur, S.; Tytgat, J. *Front. Pharmacol.* **2011**, *2*, 71.
(9) Borcsa, B.; Fodor, L.; Csupor, D.; Forgo, P.; Molnár, A., V; Hohmann, J. *Planta Med.* **2014**, *80*, 231.
(10) Wang, F.-P.; Chen, Q.-H. The C$_{19}$-Diterpenoid Alkaloids. In *The Alkaloids: Chemistry and Biology*; Cordell, G. A., Ed.; Academic Press: San Diego, 2010; Vol. 69, pp 1–577.
(11) Wang, F.-P.; Liang, X.-T. C$_{20}$-Diterpenoid Alkaloids. In *The Alkaloids: Chemistry and Biology*; Cordell, G. A., Ed. Academic Press: San Diego, 2002; Vol. 59, pp 1–280.
(12) Marth, C. J.; Gallego, G. M.; Lee, J. C.; Lebold, T. P.; Kulyk, S.; Kou, K. G. M.; Qin, J.; Lilien, R.; Sarpong, R. *Nature* **2015**, *528*, 493.
(13) Kou, K. G. M.; Li, B. X.; Lee, J. C.; Gallego, G. M.; Lebold, T. P.; DiPasquale, A. G.; Sarpong, R. *J. Am. Chem. Soc.* **2016**, *138*, 10830.
(14) Pelletier, S. W.; Parthasarathy, P. C. *Tetrahedron Lett.* **1963**, *4*, 205.
(15) For early formal syntheses of atisine, see: (a) Nagata, W.; Sugasawa, T.; Narisada, M.; Wakabayashi, T.; Hayase, Y. *J. Am. Chem. Soc.* **1963**, *85*, 2342. (b) Nagata, W.; Sugasawa, T.; Narisada, M.; Wakabayashi, T.; Hayase, Y. *J. Am. Chem. Soc.* **1967**, *89*, 1483. (c) Masamune, S. *J. Am. Chem. Soc.* **1964**, *86*, 291. (d) Guthrie, R. W.; Valenta, Z.; Wiesner, K. *Tetrahedron Lett.* **1966**, *7*, 4645.
(16) Masamune, S. *J. Am. Chem. Soc.* **1964**, *86*, 290.
(17) (a) Nagata, W.; Narisada, M.; Wakabayashi, T.; Sugasawa, T. *J. Am. Chem. Soc.* **1964**, *86*, 929. (b) Nagata, W.; Narisada, M.; Wakabayashi, T.; Sugasawa, T. *J. Am. Chem. Soc.* **1967**, *89*, 1499.
(18) (a) Wiesner, K.; Uyeo, S.; Philipp, A.; Valenta, Z. *Tetrahedron Lett.* **1968**, *9*, 6279. (b) Wiesner, K.; Komlossy, Z. I.; Philipp, A.; Valenta, Z. *Experientia* **1970**, *26*, 471.
(19) For a review on the total syntheses of diterpenoid alkaloids, see: Zhu, G.; Liu, R.; Liu, B. *Synthesis* **2015**, *47*, 2691.
(20) For a review on the use of the oxidative dearomatization/Diels−Alder cycloaddition sequence for the synthesis of diterpenes and diterpenoid alkaloids, see: Liu, X.-Y.; Qin, Y. *Nat. Prod. Rep.* **2017**, Advance Article, doi: 10.1039/C7NP00033B.
(21) Cherney, E. C.; Lopchuk, J. M.; Green, J. C.; Baran, P. S. *J. Am. Chem. Soc.* **2014**, *136*, 12592.
(22) Cheng, H.; Zeng, F.-H.; Yang, X.; Meng, Y.-J.; Xu, L.; Wang, F. P. *Angew. Chem., Int. Ed.* **2016**, *55*, 392.
(23) Hamlin, A. M.; Cortez, F. de J.; Lapointe, D.; Sarpong, R. *Angew. Chem., Int. Ed.* **2013**, *52*, 4854.
(24) Hamlin, A. M.; Lapointe, D.; Owens, K.; Sarpong, R. *J. Org. Chem.* **2014**, *79*, 6783.
(25) Nishiyama, Y.; Han-ya, Y.; Yokoshima, S.; Fukuyama, T. *J. Am. Chem. Soc.* **2014**, *136*, 6598.
(26) Nishiyama, Y.; Yokoshima, S.; Fukuyama, T. *Org. Lett.* **2016**, *18*, 2359.
(27) Corey, E. J.; Howe, W. J.; Orf, H. W.; Pensak, D. A.; Petersson, G. *J. Am. Chem. Soc.* **1975**, *97*, 6116.

(28) For a book chapter on connectivity analysis, see: Wender, P. A.; Miller, B. L. Toward the Ideal Synthesis: Connectivity Analysis and Multi-Bond Forming Processes. In *Organic Synthesis: Theory and Applications*; Hudlický, T., Ed.; JAI Press Inc.: Greenwich, CT, 1993; Vol. 2, pp. 27–66.

(29) Corey, E. J.; Cheng, X.-M. *The Logic of Chemical Synthesis*; Wiley: Hoboken, NJ, 1989; pp. 43–44.

(30) Hoffmann, R. W. *Elements of Synthesis Planning*; Springer-Verlag: Berlin, 2009.

(31) See SI for an example with weisaconitine D (**2**).

(32) Steinbeck, C.; Han, Y.; Kuhn, S.; Horlacher, O.; Luttmann, E.; Willighagen, E. L. *J. Chem. Inf. Comput. Sci.* **2003**, *43*, 493.

(33) Steinbeck, C.; Hoppe, C.; Kuhn, S.; Floris, M.; Guha, R.; Willighagen, E. L. *Curr. Pharm. Des.* **2006**, *12*, 2111.

(34) The web-based graphing program that we developed is available at http://www.cadrerl.com/maxbridge.

(35) Streit, U.; Bochet, C. G. *Beilstein J. Org. Chem.* **2011**, *7*, 525.

(36) Avent, A. G.; Byrne, P. W.; Penkett, C. S. *Org. Lett.* **1999**, *13*, 2073.

(37) Wang, Q.; Chen, C. *Org. Lett.* **2008**, *10*, 1223.

(38) Adams, H.; Anderson, J. C.; Bell, R.; Jones, D. N.; Peel, M. R.; Tomkinson, N. C. *J. Chem. Soc. Perkin Trans. 1* **1998**, 3967.

(39) Prabhakaran, J.; Lhermitte, H.; Das, J.; Sasi-Kumar, T. K.; Grierson, D. S. *Synlett* **2000**, 658.

(40) Lebold, T. P.; Gallego, G. M.; Marth, C. J.; Sarpong, R. *Org. Lett.* **2012**, *14*, 2110.

(41) Bandyopadhyaya, A. K.; Manion, B. D.; Benz, A.; Taylor, A.; Rath, N. P.; Evers, A. S.; Zorumski, C. F.; Mennerick, S.; Covey, D. F. *Bioorg. Med. Chem. Lett.* **2010**, *20*, 6680.

(42) Takaya, Y.; Ogasawara, M.; Hayashi, T. *Tetrahedron Lett.* **1999**, *40*, 6957.

(43) Lee, J.; Kim, M.; Chang, S.; Lee, H.-Y. *Org. Lett.* **2009**, *11*, 5598.

(44) Nuss, J. M.; Chinn, J. P.; Murphy, M. M. *J. Am. Chem. Soc.* **1995**, *117*, 6801.

(45) Wenkert, E. *Chem. Ind. (London)* **1955**, 282.

(46) Coates, R. M.; Bertram, E. F. *J. Org. Chem.* **1971**, *36*, 3722.

(47) Adams, M. R.; Bu'Lock, J. D. *J. Chem. Soc., Chem. Commun.* **1975**, 389.

(48) Lupi, A.; Patamia, M.; Grgurina, I.; Bettolo, R. M.; Leo, O. D.; Gioia, P.; Antonaroli, S. *Helv. Chim. Acta.* **1984**, *67*, 2261.

(49) Doering, W. v. E.; Farber, M. *J. Am. Chem. Soc.* **1949**, *71*, 1514.

(50) For a review on the synthesis of bicyclo[3.2.1]octanes, see: Filippini, M.-H.; Rodriguez, J. *Chem. Rev.* **1999**, *99*, 27.

(51) Wiesner, K.; Tsai, T. Y. R.; Huber, K.; Bolton, S. E. *J. Am. Chem. Soc.* **1974**, *96*, 4990.

(52) Wiesner, K.; Tsai, T. Y. R.; Nambiar, K. P. *Can. J. Chem.* **1978**, *56*, 1451.

(53) Cheng, H.; Xu, L.; Chen, D.-L.; Chen, Q.-H.; Wang, F.-P. *Tetrahedron* **2012**, *68*, 1171.

(54) DFT calculations suggest that the observed DMSO-adduct is 5.0–6.4 kcal/mmol lower in energy than the alternative DMSO-adducts formed via an S_N2' addition onto the carbocation intermediate. See SI for details.

(55) (a) Fernández, I.; Cossío, F. P.; Sierra, M. A. *Chem. Rev.* **2009**, *109*, 6687. (b) Hugelshofer, C. L.; Magauer, T. *Nat. Prod. Rep.* **2017**, *34*, 228. (c) Santalla, H.; Faza, O. N.; Gómez, G.; Fall, Y.; López, C. S. *Org. Lett.* **2017**, *19*, 3648.

(56) Zhao, D.-K.; Ai, H.-L.; Zi, S.-H.; Zhang, L.-M.; Yang, S.-C.; Guo, H.-C.; Shen, Y.; Chen, Y.-P.; Chen, J.-J. *Fitoterapia* **2013**, *91*, 280.

(57) Wang, F.-P.; Chen, Q.-H.; Liu, X.-Y. *Nat. Prod. Rep.* **2010**, *27*, 529.

(58) Cuerva, J. M.; Campaña, A. G.; Justicia, J.; Rosales, A.; Oller-López, J. L.; Robles, R.; Cárdenas, D. J.; Buñuel, E.; Oltra, J. E. *Angew. Chem., Int. Ed.* **2006**, *45*, 5522.

(59) Xie, G.-B.; Chen, Q.-H.; Chen, D.-L.; Jian, X.-X.; Wang, F.-P. *Heterocycles* **2003**, *60*, 631.

(60) A related, two-step, aldol-NaBH(OAc)$_3$ reduction sequence was used to install a hydroxymethyl group at the C4 position in a study toward acochlearine: Fujioka, K.; Miyamoto, N.; Toya, H.; Okano, K.; Tokuyama, H. *Synlett* **2016**, *27*, 621.

(61) Drosos, N.; Morandi, B. *Angew. Chem., Int. Ed.* **2015**, *54*, 8814.

(62) Barton, D. H. R.; Subramanian, R. *J. Chem. Soc., Perkin Trans. 1*, **1977**, 1718.

(63) Tom, N. J.; Simon, W. M.; Frost, H. N.; Ewing, M. *Tetrahedron Lett.* **2004**, *45*, 905.

(64) Holder, R. W.; Matturro, M. G. *J. Org. Chem.* **1977**, *42*, 2166.

(65) Radivoy, G.; Alonso, F.; Moglie, Y.; Vitale, C.; Yus, M. *Tetrahedron* **2005**, *61*, 3859.

(66) Corey, E. J.; Chaykovsky, M. *J. Am. Chem. Soc.* **1965**, *87*, 1353.

(67) Weitz, E.; Scheffer, A. *Ber. Dtsch. Chem. Ges. B* **1921**, *54*, 2327.

(68) Tang, P.; Chen, Q.-F.; Wang, L.; Chen, Q.-H.; Jian, X.-X.; Wang, F.-P. *Tetrahedron* **2012**, *68*, 5668.

(69) Willoughby, P. H.; Jansma, M. J.; Hoye, T. R. *Nat. Protoc.* **2014**, *9*, 643.

(70) Kolak, U.; Öztürk, M.; Özgökçe, F.; Ulubelen, A. *Phytochemistry* **2006**, *67*, 2170.

(71) Wada, K.; Kawahara, N. *Helv. Chim. Acta* **2009**, *92*, 629.

(72) Díaz, J. G.; Ruiza, J. G.; Herz, W. *Phytochemistry* **2005**, *66*, 837.

(73) Yusupova, I. M.; Bessonova, I. A.; Tashkodzhaev, B. *Chem. Nat. Compd.* **1995**, *31*, 228.

(74) Schotes, C.; Mezzetti, A. *J. Am. Chem. Soc.* **2010**, *132*, 3652.

(75) Schotes, C.; Althaus, M.; Aardoom, R.; Mezzetti, A. *J. Am. Chem. Soc.* **2012**, *134*, 1331.

(76) Oyama, H.; Orimoto, K.; Niwa, T.; Nakada, M. *Tetrahedron: Asymmetry.* **2015**, *26*, 262.

(77) Orimoto, K.; Oyama, H.; Namera, Y.; Niwa, T.; Nakada, M. *Org. Lett.* **2013**, *15*, 768.

Bioinspired strategy allows access to C_{18}, C_{19}, and C_{20} diterpenoid alkaloids

cochlearenine (C_{20})

liljestrandinine (C_{19})

weisaconitine D (C_{18})